International Journal of Advance Research and Innovation
Vol. 5(1), Jan-Mar 2017, pp. 193-201
Doi: 10.51976/ijari.511731

Article Info
Received: 25 Jan 2017 | Revised Submission: 20 Feb 2017 | Accepted: 28 Feb 2017 | Available Online: 15 Mar 2017

Impact of Clearance Contact on the Performance of Hydrodynamic Journal Bearing System

Harpreet Singh Bitta1, Gobind Pal1**, RKAwasthi***, Manjeet Singh Minhas****, Davinder Singh*****, Navneet Singh******, Vijay Kumar******* amd Keshwer Equbal Khan*********

ABSTRACT

The paper presents the analytical study of the impact of clearance contact on hydrodynamic journal bearing system's static performance. The governing model of hydrodynamic lubrication i.e. the non-dimensional Reynolds equation is solved with using Garlerkin's FEM approach along with appropriate boundary conditions. A cavitation zone, which is unknown priori is established using Reynolds boundary condition through iteratively. A clearance parameter is described and its influence on fluid-film pressure and static performance parameters of hydrodynamic journal bearing is studied for a commonly used range of sommerfeld number. The static performance parameters include maximum pressure, load carrying capacity, attitude angle, and coefficient of fluid-film friction etc. The results of the study are useful to the bearing designer from the view point of static performance parameters as the effect of sommerfeld number has been used for commonly used clearance parameter.

Keywords: *Hydrodynamic Journal Bearing; Static Characteristics; Finite Element Method.*

1.0 Introduction

The use of hydrodynamic journal bearing is in a large number of rotating machineries. In this bearing the position of journal is directly related to external load.

As the load increases, the journal shifts eccentrically, forming a wedge shaped oil film. This action of the film causes load supporting pressure, commonly known as "hydrodynamic fluid-film pressure".

The fluid-film pressure and bearing performance is influenced by various operating and geometric design parameters. Amongst these design parameter, radial clearance is an essentially invariant and its influence has been studied by several investigations.

The use of hydrodynamic journal bearing is in a large number of rotating machineries. In this bearing the position of journal is directly related to external load.

As the load increases, the journal shifts eccentrically, forming a wedge shaped oil film. This action of the film causes load supporting pressure, commonly known as "hydrodynamic fluid-film pressure".

The fluid-film pressure and bearing performance is influenced by various operating and geometric design parameters.

Amongst these design parameter, radial clearance is an essentially invariant and its influence has been studied by several investigations.

**Corresponding Author: Department of Mechanical Engineering, BCET Gurdaspur, Punjab-143521 India (E-mail: harpreet.s.bitta@gmail.com)*
***Department of Mechanical Engineering, BCET Gurdaspur, Punjab-143521 India*
****Department of Mechanical Engineering, BCET Gurdaspur, Punjab-143521 India*
*****Department of Mechanical Engineering, BCET Gurdaspur, Punjab-143521 India*
******Department of Mechanical Engineering, ST Soldier College of Engineering and Technology, Jalandhar, Punjab, India*
*******Department of Mechanical Engineering, ST Soldier College of Engineering and Technology, Jalandhar, Punjab, India*
********Department of Mechanical Engineering, BCET Gurdaspur, Punjab-143521 India*
*********Department of Mechanical Engineering, BCET Gurdaspur, Punjab-143521 India*

Ocvirk and Dubois [1] examined that load carrying capacity decreases with increase in bearing clearance and the peak pressure in the oil film rises rapidly with eccentricity ratio and with increasing bearing clearance. Mitsui et al.[2] examined that the bearing surface temperature rise increaseswith decreasing the radial clearance. Prasad [3] studied the effect of clearance ratio on the maximum bearing temperature and its location, the surface temperature rise increases with decreasing of radial clearance. Simmsons and Dixon [4] showed that the results for the large clearance configurations did not show the dramatic variation in maximum bearing temperature associated with a transition from laminar to turbulent cooling that was found for standard clearance cases.Papadopoulos et al. [5] theoretically presented the identification of clearances and stability analysis for a rotor journal bearing system using response measurements of the rotor at a particular point i.e the midpoint of the rotor. The measurements should be taken at two different speeds and from different wear effects. This present work also verified experimentally from the previous work. Sharma et al.[6] studied on the journal bearing performances and metrology issues. In this experimental study out--of-roundness and radial clearance of journal bearings were measured with high precision and the impact of their metrology was examined on the specific oil film thickness of the bearing. Results showed that the radial clearance measurements can vary from one measuring device to another and the specified clearance may not necessarily meet the design criteria of specific oil film thickness. Tian et al. [7] examined the effect of bearing outer clearance on dynamic behavior of full floating ring and observed that the stability could be enhanced by increasing clearance. Fargere and Velex [8] examined that the alignment of the shaft can be modified by changing the bearing clearance. Theoretically examine the influence of clearance parameter on the non-dimensional values of pressure distribution and static performance parameter for the bearing operating under three different values of clearance parameter. The study presents a wide operating range by choosing a commonly used values of sommerfeld number. The results of the study from the view point of clearance impact on bearing performance is useful to the bearing designer.

2.0 Analysis

In order to conduct the theoretical study, the governing two-dimensional steady state Reynolds equation is solved making the use of finite element method (FEM) for evaluating pressure distribution. The details of the analysis are presented in the following sections. In Subsection 2.1, non-dimensional Reynolds equation and fluid-film thickness is expressed.

Whereas Subsection 2.2 [9], discuss FEM formulation for converting a partial differential equation into system equation. Subsection 2.3 describes the boundary conditions and details about Reynolds boundary condition. Subsection 2.4 describes the static performance parameter which are obtained in numerical simulation.

2.1 Reynolds equation

For the analysis purpose, a two dimensional Reynolds equation for hydrodynamic lubrication in terms of cartesian cordinates is expressed as

$$\frac{\partial}{\partial x}\left(\frac{h^3}{12\mu}\frac{\partial p}{\partial x}\right)+\frac{\partial}{\partial y}\left(\frac{h^3}{12\mu}\frac{\partial p}{\partial y}\right)=\frac{u}{2}\frac{\partial h}{\partial x} \quad (1)$$

where the fluid-film thickness, h is expressed as [2]

$$h = c - x_j \cos\alpha - z_j \sin\alpha \quad (2)$$

The equation (1) reduces to the following non-dimensional form which is expressed as

$$\frac{\partial}{\partial \alpha}\left(\frac{\bar{h}^3}{12\mu}\frac{\partial \bar{p}}{\partial \alpha}\right)+\frac{\partial}{\partial \beta}\left(\frac{\bar{h}^3}{12\mu}\frac{\partial \bar{p}}{\partial \beta}\right)=\frac{\Omega}{2}\frac{\partial \bar{h}}{\partial \alpha} \quad (3)$$

Where from equation (2), a non-dimensional value of h is expressed as

$$\bar{h} = \bar{c} - \bar{x}_j \cos\alpha - \bar{z}_j \sin\alpha \quad (4)$$

The clearance parameter $\bar{c}$ is expressed as the ratio of actual clearance to the reference clearance. The clearance contact is described in terms of non-dimensional clearance parameter $\bar{c}$.

2.2 FEM components

The fluid flow inside the clearance space of finite journal bearing as described by Eq [3] is solved using FEM. The entire domain is descretised by making use of four noded quadrilateral isoperimetric elements. Using Lagrangian linear interpolation function, the pressure within the element is bilinearly distributed and approximated as

$$\left.\begin{aligned} \bar{p} &= \sum_{j=1}^{4} \bar{p}_j \bar{N}_j \\ \alpha &= \sum_{j=1}^{4} N_j \alpha_j \\ \beta &= \sum_{j=1}^{4} N_j \beta_j \\ \frac{\partial p}{\partial \alpha} &= \sum_{j=1}^{4} \frac{\partial N_j}{\partial \alpha} \cdot \bar{p}_j \\ \frac{\partial p}{\partial \beta} &= \sum_{j=1}^{4} \frac{\partial N_j}{\partial \beta} \cdot \bar{p}_j \end{aligned}\right\} \quad (5)$$

where N_j is Lagrangian interpolation function.

Using Garkelin's orthogonally criteria using approximate equivalent of p, equation (3) can be expressed as

$$\frac{\partial}{\partial x}\left[\frac{\bar{h}^3}{12\bar{\mu}}\frac{\partial}{\partial \alpha}\left(\sum_{j=1}^{4} P_j N_j\right)\right] + \frac{\partial}{\partial \beta}\left[\frac{\bar{h}^3}{12\bar{\mu}}\frac{\partial}{\partial \beta}\left(\sum_{j=1}^{4} P_j N_j\right)\right] - \Omega\left[\frac{1}{2}\frac{\partial \bar{h}}{\partial \alpha}\right] = R^e \quad \ldots \quad (6)$$

Where R^e is known as residue of element, minimization of residue is brought by means of ortogonalising the residue with interpolation features, i.e.

$$\iint_{\Omega e} N_j R^e \, d\alpha.d\beta = 0 \quad \ldots (7)$$

Integrating the 2nd order term in equation (7) by the way of elements acquire c^o continuity, the resultants equation for a typical e^{th} element is brought in matrix form as follows

$$[\bar{F}]^e\{\bar{p}\}^e = \{\bar{Q}\}^e + \Omega\{\bar{R}_H\}^e \quad \ldots (8)$$

For e^{th} element, the matrix and coulumn-vectors are considered as

$$\bar{F}^e{}_{ij} = \iint_{\bar{A}^e}\left\{\frac{\bar{h}^3}{12\bar{\mu}}\left(\frac{\partial N_i}{\partial \alpha}\frac{\partial N_j}{\partial \alpha} + \frac{\partial N_i}{\partial \beta}\frac{\partial N_j}{\partial \beta}\right)\right\} d\alpha \, d\beta \quad (9a)$$

$$\bar{Q}^e{}_i = \int_{\tau^e}\left\{\left(\frac{\bar{h}^3}{12\bar{\mu}}\frac{\partial \bar{p}}{\partial \alpha} - \frac{1}{2}\bar{\Omega}\bar{h}\right) l_1 + \left(\frac{\bar{h}^3}{12\bar{\mu}}\frac{\partial \bar{p}}{\partial \bar{\beta}}\right) l_2\right\} N_i \, d\bar{\tau}^e \quad (9b)$$

$$\bar{R}^e{}_{Hi} = \iint_{\bar{A}^e} \frac{1}{2}\bar{h}\frac{\partial N_i}{\partial \alpha} \, d\alpha \, d\beta \quad (9c)$$

Where l_1 and l_2 are direction cosines and i,j = 1,2……$n_j{}^e$ are number of nodes per element.

A^e refers area and τ^e is the boundary of the eth element.

After usual assembly procedure, global system equation is obtained as

$$[\bar{F}]\{\bar{P}\} = [\bar{Q}] + \Omega\{R_H\} \quad \ldots (9)$$

2.3 Boundary conditions

For small disturbances, the extent of positive pressure film may be assumed to remain unchanged. It may be noted that the boundary of positive pressure zone is unknown, which is established by considering the cavitated pressure to be constant and equal to be zero. In order to achieve the consistency in cavitated pressure zone, the pressure gradient is also been considered to be zero, therefore the following boundary conditions may be stipulated.

1. At the external boundary, nodal pressure are zero,

$$\bar{p}.(\alpha,\beta = \pm 1.0) = 0.0 \quad \ldots (10a)$$

2. At the trailing edge of positive pressure region, and Reynolds boundary condition $\bar{p}(\alpha_2,\beta) = 0$,

$$\frac{\partial \bar{p}}{\partial \alpha} = \frac{\partial \bar{p}}{\partial \beta} \quad \ldots (10b)$$

2.4 Static performance parameters

The dimensionless fluid-film force on the journal surface is given by

$$\left.\begin{aligned} \bar{F}_x &= \int_{-1}^{1}\int_{0}^{2\pi} \bar{p}\cos\alpha.d\alpha.d\beta \\ \bar{F}_z &= \int_{-1}^{1}\int_{0}^{2\pi} \bar{p}\sin\alpha.d\alpha.d\beta \end{aligned}\right\} \quad \ldots (11)$$

And the resultant fluid-film force F, is equivalent to force $\bar{F} = \sqrt{F_x{}^2 + F_z{}^2}$

Sommerfeld number

A more commonly used quantity to describe the load characteristics of a journal bearing is the Sommerfeld number. In the design of fluid bearing the Sommerfeld number or bearing characteristic number, is a dimensionless quantity extensively in hydrodynamic lubrication analysis. The Sommerfeld number is very important in lubrication analysis because it contain all the variables. The Sommerfeld number is typically defined by the following equation

$$S = \left(\frac{R}{c_o}\right)^2 \frac{\mu N}{P}$$

S is the Sommerfeld number

r is the journal radius

c_0 is the Reference radial clearance

μ is the absolute viscosity of the lubricant

N is the speed of the rotating journal in r.p.m

P is the load per unit projected bearing area or pressure

The non-dimensional hydrodynamic friction force in a journal bearing is calculated as

$$\bar{F}_f = \sum_{e=1}^{n_e}\int_{A^e}\left[\frac{1}{\bar{h}} + \left(\frac{\bar{h}}{2}\frac{\partial \bar{P}}{\partial \alpha}\right)\right] d\bar{A}_e \quad \ldots (12)$$

Where n_e total number of elements in fluid-flow domain.

The coefficient of friction of fluid-film is given by

$$f\left(\frac{R}{c_o}\right) = \frac{\bar{F}_f}{\bar{F}} \quad \ldots (13)$$

Attitude angle

The vicinity of journal centre is measured by using attitude angle which is the angle shaped between the vertical and a line that crosses via the centre of the journal and the centre of the bearing. The attitude angle is calculated as

$$ø = \tan^{-1}\left|\frac{\bar{x}_j}{\bar{z}_j}\right|$$

End leakage

The bearing end flow is expressed as The sum of all nodal flow. The internal nodes having zero flow, as the flow entering and exit corresponding to the particular node is same. The expression for end leakage is described as

$$\overline{Q} = \sum_{e=1}^{ne} \overline{Q}^e \quad \ldots (14)$$

3.0 Solution Procedure

The solution of hydrodynamic journal bearing requires an iterative scheme at two stages. In order to establish the ($\bar{p}$> 0) pressure zone, which is unknown priori, iteration is needed. Further the pressure area is computed for a specific value of attitude angle at a specified eccentricity.

The solution scheme uses various modules as shown in figure 1, the iteration continues until a journal equilibrium is attained for a designated eccentricity ratio.

The study of clearance contact through numerical simulation with FEM is involved process and the computational procedure is shown in Fig.1. The numerical procedure contains the following steps:

1. The fluid-film domain of journal bearing is automatically discretized into 4 noded quadrilateral elements in circumferential and axial direction, as shown in Fig.1.
2. Fluid film pressure distribution field are initialised by assigning an arbitrary value of journal centre.
3. Fluid-film thickness is calculated using eq. (4).
4. A two points Guass quadrature is used for the integration in elements. Thus four Gauss points are generated in our isoparametric quadrilateral n element.
5. Elements equations are assembled using indexing to obtain global system of matrices and then boundary conditions are implemented.
6. Cavitated boundaries, which are unknown priori is established using ref. (11).
7. Fluid-film reaction is computed using numerical integration of nodal pressure in Eq.(11).
8. At a specified eccentricity, the attitude angle is fixed which is obtained using Newton's iteratve method.
9. Steps 3-9 are repeated until convergence is achieved. The algorithm uses $\left|\frac{F_x}{F}\right| \leq 0.1\%$, to achieve the convergence.
10. Once the above convergence criteria is satisfied, static performance characteristics are computed using the expressions described in earlier sections.

4.0 Results and Discussion

Based on the flow chart and solution procedure discussed, a computer code utilising MATLAB is developed. The current study uses a grid independent mesh (36×8), to describe the fluid-film domain. The selection of grid size is based on the accuracy of simulated data and minimum computational time.

The simulated influence from the present gain knowledge of is when put next with the released results of Raimondi and Boyd [10], Chandrawat and Sinhasan [11] and Jain et al.[12].

Table 1 Analysis of Static Characteristics of Plain Journal Bearing (Eccentricity Ratio $\varepsilon = 0.6$, L/D =1)

Performance Parameters	Current Work	Raimondi and Boyd Ref. (10)	Chandrawat and Sinhasan Ref. (11)
Load Capacity, $\overline{W}_0$	5.095	5.2613	5.1662
Attitude Angle, ϕ	52.044	50.58	51.99
Friction coefficient	3.319	3.22	3.41

Fig 1: Flow Chart of Solution Scheme

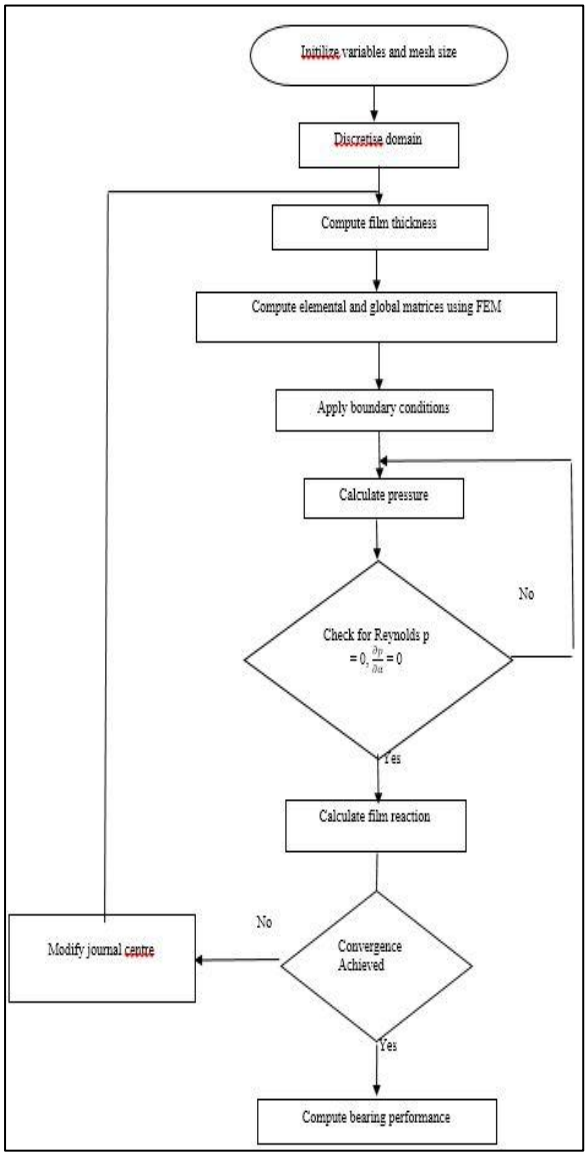

For clearance parameter $\bar{c}$ = 1.0, ε = 0.6 and 0.7. The comparisons of computed data are presented in Tables 1 and 2. It may be observed from these tables that the results from the current study is in good agreement from the published data with a maximum deviation is less than 2%.The simulated results presented in Tables 1 and 2, establishes the accuracy of developed code. The numerically simulated results from the developed model is awarded for fluid-film pressure distribution along circumferential and axial direction for the commonly used operating parameters ε = 0.5. The bearing configuration in the current study is considered to be finite one.

The clearance parameters for the non-dimensional pressure and fluid-film thickness are taken to be $\bar{c}$= 1.0, 1.2, 1.4.

Table 2 Comparison of Static Characteristics of Plain Journal Bearing (Eccentricity Ratio $\varepsilon = 0.7$, L/D =1)

Performance Parameters	Current Work	Jain et al. Ref. (12)	Chandrawat and Sinhasan Ref. (11)
Minimum Fluid-Film Thickns, $\bar{h}_{min}$	0.303	0.300	0.300
Maximum Fluid-Film Press. $\bar{p}_{max}$	5.478	5.360	5.516
Load Capacity, $\bar{W}_0$	7.889	7.66	7.98
Attitude Angle, ϕ	45.104	43.66	44.97
Friction coefficient	2.478	2.5457	2.4524

Figure 2 represents the relation between the maximum pressure and circumferential direction. Figure represents the pressure profile at different clearance parameter resulting the fluid-film journal bearing achieve a higher value at small clearance parameter.

From the figure it is clear that from α = 0 to 130^0 oil film pressure is zero. From α = 130^0 pressure starts rising and becomes maximum near to α = 290^0 and then falls at α = 300^0. A decrease in clearance parameter yields the pressure profile rise, which is tending to increase in hydrodynamic action.

Figure 3 represents as the clearance parameter increases the overall fluid-film thickness also increases. It shows that the bearing is unwrapped, the fluid film thickness start increasing up to 160^0, which is top segment of bearing whereas it start decreasing at the bottom segment and then slightly increasing up to 360^0.

Figure 4 shows that pressure is maximum at centre of bearing. Figure represent that at relative clearance 1.0, the pressure becomes maximum and as the relative clearance increases up to 1.4 pressure decreases.

4.1 Static performance parameters

From the previous study, it is clear that the lower value of clearance parameter shows better bearing static performance.

In order to have more insight, the current section compares roto-static performance clearance parameter $\bar{c}$ =1.0, 1.2 and 1.4. From the generated knowledge, the bearing performance characteristics has been plotted as a perform of clearance parameter $\bar{c}$.

Fig 2: Influence of Clearance Parameters in Pressure Distributions in Circumferential Direction

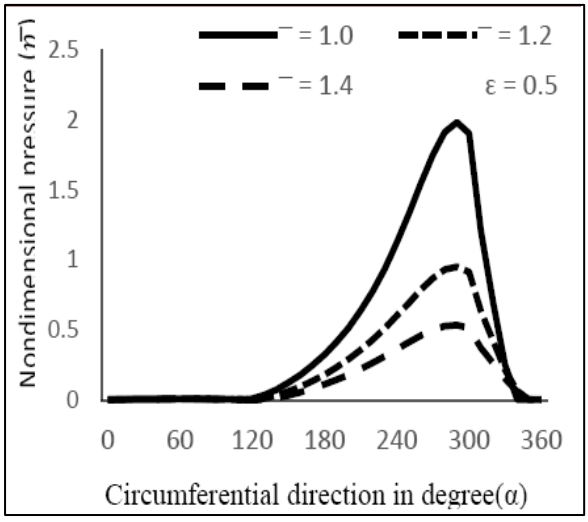

Fig.3 Influence of Clearance Parameter on Fluid Film Thickness in Circumferential Direction

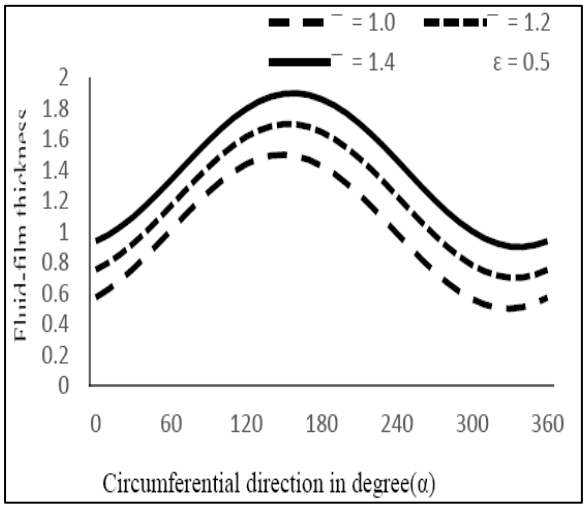

Fig 4: Film Thickness in Axial Direction

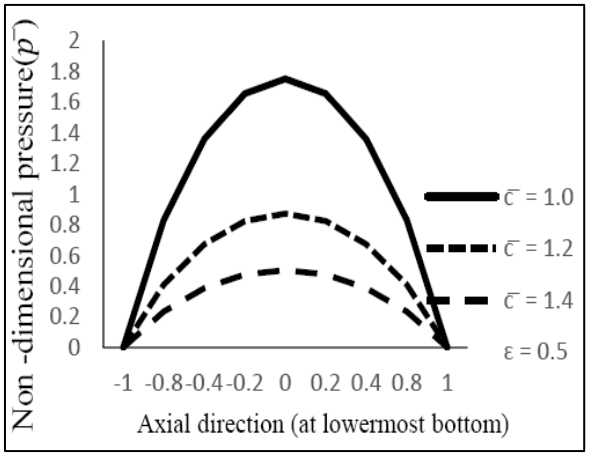

4.1.1 Influence on maximum pressure ($\bar{P}$max)

Figure 5 shows that maximum pressure is increased by increasing the value of clearance parameter. At higher value of Sommerfeld number (S) and higher value of clearance parameter ($\bar{c}$ = 1.4) the maximum pressure has minimum value.

When the value of Sommerfeld number (S) as well as clearance parameter is increasing then the value of maximum pressure is decreasing. The value of maximum pressure is maximum at ($\bar{c}$ = 1.4).

4.1.2 Influence on attitude angle (ø)

Figure 6 shows that at minimum value of clearance parameter ($\bar{c}$ = 1.0) and maximum value of Sommerfeld number (S) the attitude angle has higher value at clearance parameter ($\bar{c}$ = 1.0). Higher the attitude angle is an indicator of minimum fluid-film thickness.

4.1.3 Influence on minimum fluid-film thickness ($\bar{h}_{min}$)

Figure 7 shows that minimum fluid-film thickness increases with the increase in the Sommerfeld number. At higher value of Sommerfeld number (S) and higher value of clearance parameter ($\bar{c}$ = 1.4) the minimum-fluid film thickness has maximum value.

When the value of Sommerfeld number (S) as well as clearance parameter is increasing then the value of minimum fluid-film thickness is increasing. The value of minimum fluid-film thickness is maximum at ($\bar{c}$ = 1.4).

Fig 5: Maximum Pressure Verses Sommerfeld Number at Different Clearance Parameter

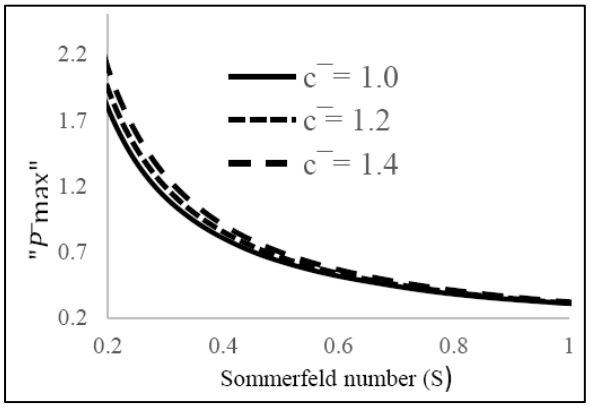

Fig 6: Attitude Angle Verses Sommerfeld Number at Different Clearance Parameter

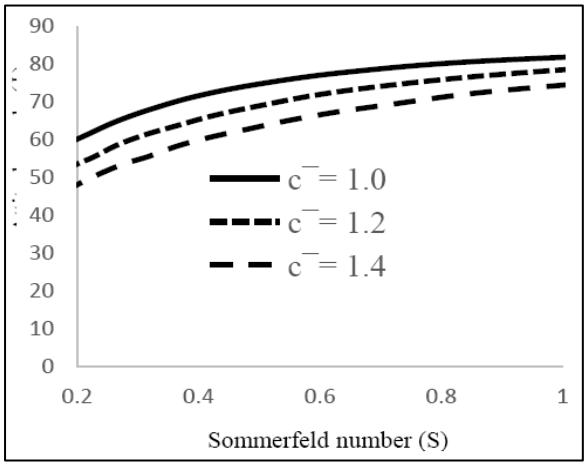

Fig 7: Minimum Fluid-Film Thickness Verses Sommerfeld Number Verses at Different Clearance Parameter

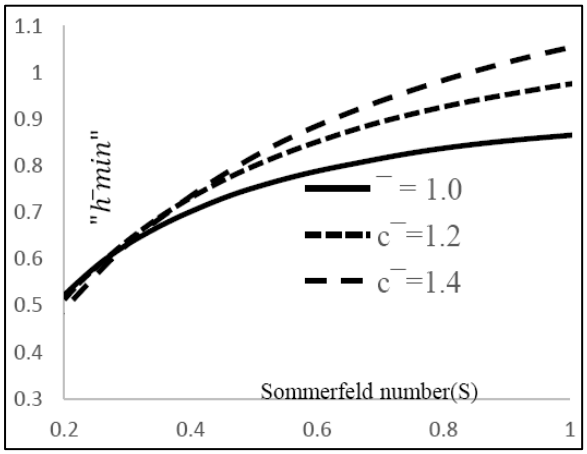

4.1.4 Effect on fluid film friction ($\bar{F}_f$) and coefficient of fluid-film friction

Figure 8shows that the value of fluid film friction is maximum at minimum value of Sommerfeld number (S) and at higher value of clearance parameter ($\bar{c}$ = 1.4). As we increase the value of Sommerfeld number (S) corresponding to clearance parameter ($\bar{c}$=1.0, $\bar{c}$= 1.2, $\bar{c}$ = 1.4) then the value of fluid-film friction is decreasing continuously. Figure 9 illustrates that the coefficient of friction increased by increasing the value of clearance parameter. At higher value of Sommerfeld number(S) and higher value of clearance parameter ($\bar{c}$ = 1.4) the coefficient of friction has maximum value. When the value of Sommerfeld number as well as clearance parameter increasing the value of coefficient of friction goes on increasing. The value of coefficient of friction is maximum at ($\bar{c}$ = 1.4).

Fig 8: Force of Friction Verses Sommerfeld Number at Different Clearance Parameter

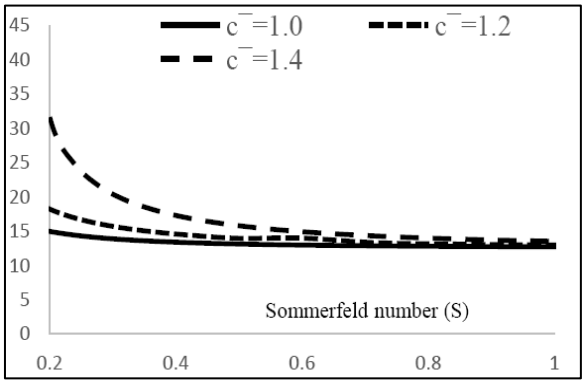

Fig 9: Coefficient of Friction Verses Sommerfeld Number at Different Clearance Parameter

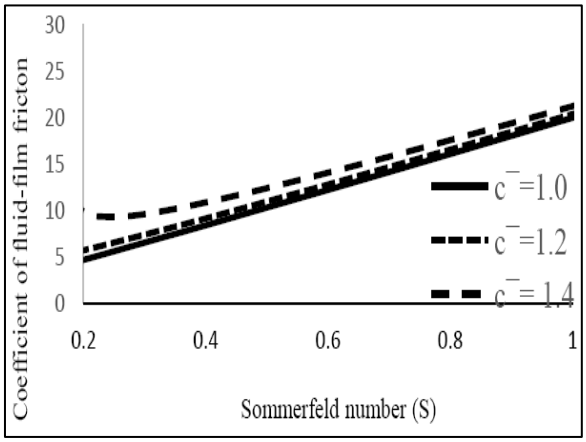

4.1.5 Effect on end leakage (Q)

Figure 10 shows that bearing side flow decreases with increase in Sommerfeld number (S) At maximum value of Sommerfeld number (S) and at maximum clearance parameter it is observed that bearing side flow has minimum value.

Fig 10: Bearing Side Flow Verses Sommerfeld Number at Different Clearance Parameter

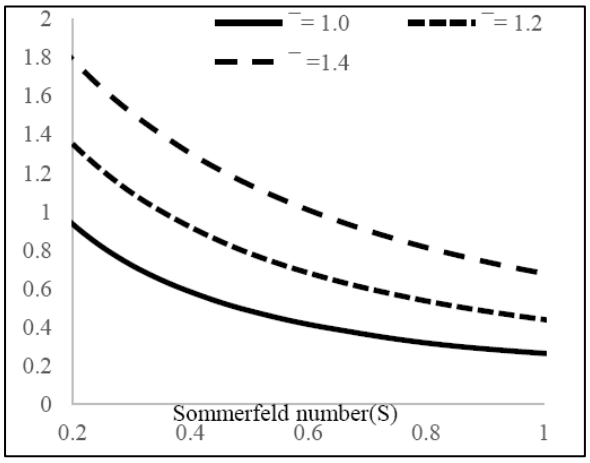

5.0 Conclusions

This work presents the theoretical study conducting the effect of clearance on the pressure, film thickness and static performance parameters of fluid film journal bearing system. Based on the numerically simulated outcomes following conclusions are drawn.

1) The maximum fluid film pressure and end flow decrease with the increase in the clearance parameters.
2) The attitude angle, coefficient of friction and minimum fluid-film thickness increases with the increases in the clearance parameters.

Nomenclature

Dimensional parameters

x,y,z co-ordinate axes with origin at geometric centre of bearing

x_j, z_j journal centre position from geometric centre of bearing

h fluid-film thickness

μ viscosity of lubricant

μ_r reference viscosity

ω angular speed of journal (rad/s)

c radial clearance

c_0 reference clearance

U tangential journal speed (ωR)

R journal radius

Non-Dimensional Parameters

α circumferential co-ordinate $\left(\frac{X}{R}\right)$

β axial xo-ordinate $\left(\frac{y}{R}\right)$

Ω speed parameter, $\frac{\omega}{\omega_r}$

$\bar{\mu} = \frac{\mu}{\mu_r}$ $\bar{\mathbf{p}} = \frac{p}{\mu\omega\left(\frac{R}{c_o}\right)^2}$

$\bar{h} = \frac{h}{c_o}$

c̄clearance parameter, $\frac{c}{c_o}$

εeccentricity ratio, $\frac{e}{c_o}$

$\alpha_2$extent of positive pressure film **e**journal eccentricity

øattitude angle, radian

$\bar{\mathbf{W}} = \frac{W}{\mu\omega R^2\left(\frac{R}{c_o}\right)^2}$

References

[1.] FW Ocvirk. BDubois, Relation of journal bearing performance to minimum oil film, NACA TN 4223 1958.

[2.] J Mitsui, Y Hori, M Tanaka. Theoretical and an experimental investigation to determine the bearing metal and oil film temperature of circular journal bearings, ASME J Tribol, 108(4), 1986, 621-626,

[3.] H Prashad. The effects of viscosity and clearance on the performance of hydrodynamic journal bearings" Tribol Trans, 31, 1987, 302-309

[4.] JEL Simmsons, SJ Dixon. Effect of load direction, preload, clearance ratio, and oil flow on the performance of a 200 mm journal pad bearing" Tribol Trans, 37, 1994, 227-236.

[5.] AC Papadopoulos, G Nikolakopoulos, D Gounaris. Identification of clearances and stability analysis for a rotor-journal bearing

[6.] system, Mechanism and Machine Theory, 43, 2008, 411–426.

[7.] S Sharma, D Hargreaves, W Scott. Journal bearing performance and metrology issues, Journal of Achievements in Material and Manufacturing Engineering, 32, 2009, 98-103.

[8.] L Tian, WJ Wang, ZJ Peng. Effects of bearing outer clearance on the dynamic behaviours of the full floating ring bearing supported turbocharger rotor, Mechanical Systems and Signal Processing, 31, 2012, 155-175.

[9.] R Fargere, P Velex. Influence of clearances and thermal effects on the dynamic behavior of gear-hydrodynamic journal bearing systems, ASME J Vibration and Acoustics, 135, 2013, 061014-1-061014-16.

[10.] A Cameron. Basic lubrication theory. London. Longman, 1971.

[11.] AA Raimondi, J Boyd. A solution for the finite journal bearings and its application to analysis and design, parts 1, 2, 3, ASLE Trans, 1, 1958, 159-209.

[12.] HN Chandrawat, R Sinhasan. A comparison for hydrodynamic journal bearing problems, Wear, 119, 1987, 77-87.

[12] SC Jain, R Sinhasan, DV Singh. A study of EHD lubrication in a journal bearing eith piezoviscous lubricant, ASLE Trans, 27, 1989,168-176